

See discussions, stats, and author profiles for this publication at: <https://www.researchgate.net/publication/5995178>

Non-innocent behaviour of ancillary and bridging ligands in homovalent and mixed-valent ruthenium complexes $[A_2Ru(?-L)RuA_2]_n$, $A = 2,4$ -pentanedionato or 2-phenylazopyridine, $L_2? = 2...$

ARTICLE in DALTON TRANSACTIONS · JULY 2007

Impact Factor: 4.2 · DOI: 10.1039/B701511A · Source: PubMed

CITATIONS

23

READS

63

6 AUTHORS, INCLUDING:



Somnath Maji

Indian Institute of Technology Hyderabad

37 PUBLICATIONS 579 CITATIONS

SEE PROFILE



Mohammad Mobin Shaikh

Indian Institute of Technology Indore

325 PUBLICATIONS 5,213 CITATIONS

SEE PROFILE

Non-innocent behaviour of ancillary and bridging ligands in homovalent and mixed-valent ruthenium complexes $[A_2Ru(\mu-L)RuA_2]^n$, $A = 2,4\text{-pentanedionato}$ or $2\text{-phenylazopyridine}$, $L^{2-} = 2,5\text{-bis}(2\text{-oxidophenyl})\text{pyrazine}^\dagger$

Somnath Maji,^a Biprajit Sarkar,^b Shaikh M. Mobin,^a Jan Fiedler,^c Wolfgang Kaim^{*b} and Goutam Kumar Lahiri^{*a}

Received 31st January 2007, Accepted 12th March 2007

First published as an Advance Article on the web 4th April 2007

DOI: 10.1039/b701511a

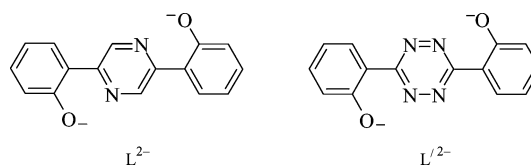
Structurally characterised 2,5-bis(2-hydroxyphenyl)pyrazine (H_2L) can be partially or fully deprotonated to form the complexes $[(acac)_2Ru(\mu-L)Ru(acac)_2]$, **[1]**, $acac^-$ = acetylacetonato = 2,4-pentanedionato, $[(pap)_2Ru(\mu-L)Ru(pap)_2](ClO_4)_2$, **[2]**, $(ClO_4)_2$, pap = 2-phenylazopyridine, or $[(pap)_2Ru(HL)](ClO_4)$, **[3]**, (ClO_4) . Several reversible oxidation and reduction processes were observed in each case and were analysed with respect to oxidation state alternatives through EPR and UV-VIS-NIR spectroelectrochemistry. In relation to previously reported compounds with 2,2'-bipyridine as ancillary ligands the complex redox system **[1]ⁿ** is distinguished by a preference for metal-based electron transfer whereas the systems **[2]ⁿ** and **[3]ⁿ** favour an invariant Ru^{II} state. Accordingly, the paramagnetic forms of **[1]ⁿ**, $n = -, 0, +$, exhibit metal-centred spin whereas the odd-electron intermediates **[2]⁺**, **[2]³⁺** and **[3]** show radical-type EPR spectra. A comparison with analogous complexes involving the 3,6-bis(2-oxidophenyl)-1,2,4,5-tetrazine reveals the diminished π acceptor capability of the pyrazine-containing bridge.

Introduction

Ligand-bridged mixed-valent metal complexes play an important role in understanding intramolecular electron transfer processes,¹ relevant *e.g.* for the designing of molecular electronic devices.^{1a,e} Thus, the discovery of pyrazine-mediated strong intermetallic electronic coupling in the mixed-valent Creutz–Taube ion $[(NH_3)_5Ru(\mu\text{-pyrazine})Ru(NH_3)_5]^{5+}$ has spurred the subsequent preparation and investigation of a large number of polyruthenium complexes encompassing pyrazine-related modified bridging ligands in combination with ancillary ligands of different electronic characteristics.² The basic perspectives of such exercises are twofold: (i) to rationalise the impact of the modified framework of pyrazine derivatives on the metal–metal coupling, and (ii) to control that interaction through external factors such as the ancillary (terminal) ligands.

In accordance with this general approach we present here two new diruthenium complexes $[(acac)_2Ru^{III}(\mu-L^{2-})Ru^{III}(acac)_2]$, **[1]**, and $[(pap)_2Ru^{II}(\mu-L^{2-})Ru^{II}(pap)_2]^{2+}$, **[2]²⁺**, which incorporate the pyrazine-derived dianionic bridging ligand $L^{2-} = 2,5\text{-bis}(2\text{-oxidophenyl})\text{pyrazine}$ ($boppz^{2-}$) in combination with σ -donating $acac^-$ ($acac^-$ = acetylacetonato = 2,4-pentanedionato) and strongly

π -acidic pap (pap = 2-phenylazopyridine) as ancillary ligands. Though ruthenium bound phenolate based bridging ligands are known,^{3a–c} bridging ligands encompassing both donor and acceptor components are less common.^{3d,4,5} The related 3,6-bis(2-oxidophenyl)-1,2,4,5-tetrazine ($boptz^{2-} = (L')^{2-}$) and its diruthenium complexes have been described recently.⁵ Such ligands are special in the sense that they can introduce a competitive situation in the complex with respect to the involvement of metal—or ligand-based—orbitals in the redox processes. This article deals with the synthetic aspects of dinuclear **[1]** and **[2]²⁺** and of mononuclear $[(pap)_2Ru^{II}(HL)]^+$, **[3]⁺**, and with assignments of metal- and ligand-based redox processes of the complexes *via* UV-VIS-NIR spectroelectrochemistry and EPR. Furthermore, the effect of the different electronic nature of the ancillary ligands, $acac^-$ or pap , towards the valence distribution and intermetallic coupling processes has been addressed in relation to the reported bipyridine (bpy)-ligated derivative $[(bpy)_2Ru^{II}(\mu-L^{2-})Ru^{II}(bpy)_2]^{2+}$, **[4]²⁺**.^{3d} Finally, a comparison with analogous complexes⁵ involving $boptz^{2-} = (L')^{2-}$ will bear on the effects of different π acceptor capability of the bridge.



The crystal structure of the protonated free ligand $H_2boppz = H_2L$ is also presented in order to confirm its identity as a pyrazine (and not a dihydropyrazine^{3d}) derivative.

^aDepartment of Chemistry, Indian Institute of Technology-Bombay, Powai, Mumbai, 400076, India. E-mail: lahiri@chem.iitb.ac.in

^bInstitut für Anorganische Chemie, Universität Stuttgart, Pfaffenwaldring 55, D-70550, Stuttgart, Germany. E-mail: kaim@iac.uni-stuttgart.de

^cJ. Heyrovsky Institute of Physical Chemistry, v.v.i., Academy of Sciences of the Czech Republic, Dolejškova 3, CZ-18223, Prague, Czech Republic

† Electronic supplementary information (ESI) available: Positive ion electrospray mass spectral data for compounds **[1]**, **[2]**, $(ClO_4)_2$ and **[3]**, (ClO_4) . See DOI: 10.1039/b701511a

Results and discussion

The starting material, the ligand 2,5-bis(2-hydroxyphenyl)pyrazine (erroneously described^{3d} as dihydropyrazine⁶) with $\delta_{\text{H}}(\text{pyrazine}) = 9.47 \text{ ppm}$,^{3d} has been crystallised for X-ray structure analysis. The result as summarised in the Experimental section and in the caption and as shown in Fig. 1 displays no unusual bond parameters, the nearly planar molecule with only $3.9(0.4)^\circ$ dihedral angles between pyrazine and the phenol rings is held in the inversion symmetrical conformation through intramolecular OH(phenol)–N(pyrazine) hydrogen bonds at 2.58 \AA N–O distance and at a calculated OHN angle of 155.0° .

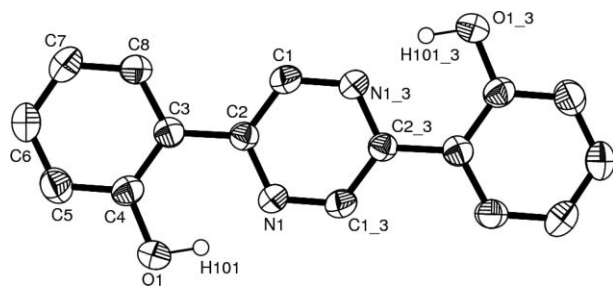
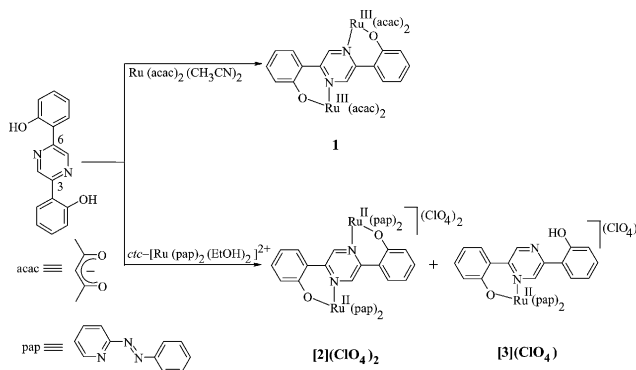


Fig. 1 Crystal structure of 2,5-bis(2-hydroxyphenyl)pyrazine. Ellipsoids are drawn at 50% probability. Essential bond lengths (\AA): N1–C1_3 1.335(4), N1–C2 1.353(4), C1–C2 1.381(5), O1–C4 1.366(4), C2–C3 1.475(4). Symmetry transformations used to generate equivalent atoms: $-x + 2, -y, -z$.

The complexes $[(\text{acac})_2\text{Ru}^{\text{III}}(\mu\text{-L}^{2-})\text{Ru}^{\text{III}}(\text{acac})_2]$, **[1]** and $[(\text{pap})_2\text{Ru}^{\text{II}}(\mu\text{-L}^{2-})\text{Ru}^{\text{II}}(\text{pap})_2](\text{ClO}_4)_2$, **[2]**(ClO_4)₂ as well as $[(\text{pap})_2\text{Ru}^{\text{II}}(\text{HL}^-)](\text{ClO}_4)$, **[3]**(ClO_4), have been synthesised *via* the reactions of (H_2L) with $\text{Ru}(\text{acac})_2(\text{CH}_3\text{CN})_2$ or *ctc*- $[\text{Ru}(\text{pap})_2(\text{EtOH})_2]^{2+}$ (*ctc* = *cis*, *trans* and *cis* with respect to ethanol, pyridine and azo nitrogen atoms, respectively⁷) in ethanol and in the presence of sodium acetate as a base (Scheme 1). Although a mononuclear product **[3]**(ClO_4) has also been formed along with the dinuclear **[2]**(ClO_4)₂ in case of $\{\text{Ru}(\text{pap})_2\}^{2+}$, only the dinuclear species **[1]** has been obtained with the $\{\text{Ru}(\text{acac})_2\}$ precursor. With bpy co-ligands the mononuclear compound, apparently containing the HL^- ligand, was also described albeit with poor elemental analysis;^{3d} sterically favoured rotation of the uncoordinated phenol substituent into a nearly orthogonal conformation relative to the Ru/phenolate/pyrazine chelate moiety could thus lead to diminished π conjugation and thus to the



Scheme 1

observed very unusual behaviour^{3d} of different LUMO character in mononuclear and dinuclear compounds. The Ru^{III} centre in the precursor $\text{Ru}(\text{acac})_2(\text{CH}_3\text{CN})_2$ has been oxidised to Ru^{III} in **[1]**. The presence of σ -donating acac^- and phenolato functions of L^{2-} in **[1]** reduces the first $\text{Ru}^{\text{III}}\text{--Ru}^{\text{II}}$ potential to -0.58 V versus SCE which stabilises the ruthenium(III) state in **[1]** under aerobic conditions. In contrast, the presence of the strongly π -accepting ancillary ligand pap in **[2]**(ClO_4)₂ and **[3]**(ClO_4) is reflected by their relatively high $\text{Ru}^{\text{III}}\text{--Ru}^{\text{II}}$ potentials at 1.05 and 0.88 V versus SCE, respectively (*cf.* below). The *ctc*-configuration of the parent $\{\text{Ru}(\text{pap})_2\}$ complex fragment is expected to be retained in **[2]**(ClO_4)₂ and **[3]**(ClO_4) (Scheme 1) as has been observed on earlier occasions.^{7b,c}

The formation of the complexes has been confirmed by positive ion electrospray mass spectral data. The compounds **[1]**, **[2]**(ClO_4)₂ and **[3]**(ClO_4) exhibit molecular mass values at 861.72 (calculated mass for **[1]**⁺, 860.85), 1297.24 (calculated mass for $\{\text{[2]}(\text{ClO}_4)_2 - \text{ClO}_4\}^+$, 1297.15) and 731.18 (calculated mass for $\{\text{[3]}(\text{ClO}_4) - \text{ClO}_4\}^+$, 730.13), respectively (Fig. S1†). The microanalytical data of the complexes agree well with the calculated values, and **[1]**, **[2]**(ClO_4)₂ and **[3]**(ClO_4) are electrically neutral, 1 : 2 and 1 : 1 conducting in CH_3CN , respectively (see Experimental section). The ruthenium(III) compound **[1]** is paramagnetic but **[2]**(ClO_4)₂ and **[3]**(ClO_4) are diamagnetic, as expected from their low-spin Ru^{II} configuration.

Complex **[1]** exhibits a magnetic moment of $2.98 \mu_{\text{B}}$ in the solid state at 298 K , corresponding to two unpaired electrons. The ^1H -NMR spectrum of paramagnetic **[1]** in CDCl_3 exhibits chemical shifts over a wide range, from 24 to -33 ppm , because of paramagnetic contact shifts (Fig. 2a, Experimental section).⁸ The unsymmetrical N,O[−] donor chelate functions of the bridging ligand make the protons associated with the ancillary ligands (acac^-) inequivalent. Thus, the mixture of *rac* and *meso* isomers of **[1]** shows ten “aromatic” protons associated with the bridging ligand L^{2-} as well as four $\text{CH}(\text{acac})$ and eight $\text{CH}_3(\text{acac})$ signals. Compound **[1]** exhibits an EPR signal at 4 K in CH_3CN [$g_1 = 2.307$, $g_2 = 2.153$ and $g_3 = 1.827$, Fig. 4a]. Both the g anisotropy ($\Delta g = g_1 - g_3$) of 0.480 and the average g ($g_{\text{av}} = [1/3(g_1^2 + g_2^2 + g_3^2)]^{1/2}$) of 2.105 are indicative of Ru^{III} .⁹ The half-field EPR signal expected for a triplet state¹⁰ has not been observed under these conditions.

The diamagnetic mononuclear (**[3]**(ClO_4)) and dinuclear (**[2]**(ClO_4)₂) species exhibit complex ^1H -NMR spectral profiles (Fig. 2b and c and Experimental section) in $(\text{CD}_3)_2\text{SO}$ due to the presence of unsymmetric ancillary (pap, $\text{N}_\text{p}/\text{N}_\text{a}$) and bridging (L^{2-} , N/O^-) chelate ligands and because of similar chemical shift values for many signals. Mononuclear **[3]**(ClO_4) exhibits 29 partially overlapping signals. Three distinct singlets due to the D_2O exchangeable free OH group and to the pyrazine protons, *meta* and *ortho* to the coordinated nitrogen centre, appear at 7.84 , 9.28 and 10.43 ppm , respectively. The dinuclear species exhibits 46 extensively overlapping signals in the range $11\text{--}6.5 \text{ ppm}$ as expected from the diastereomeric mixture (*rac* and *meso*). The CH protons of the coordinated pyrazine ring of L^{2-} appear at 11.05 ppm as a singlet.

The diruthenium(III) complex **[1]** undergoes two successive oxidation and reduction processes (Table 1, Fig. 3a). The low first $\text{Ru}^{\text{III}} = \text{Ru}^{\text{II}}$ potential at -0.58 V indicates the stabilisation of the Ru^{III} state in **[1]**. The comproportionation constant (K_c) values of the intermediates are calculated to be $10^{2.4}$ (**[1]**⁺) and $10^{5.8}$ (**[1]**[−]), calculated using the equation $RT \ln K_c = nF(\Delta E)$.^{2a} The

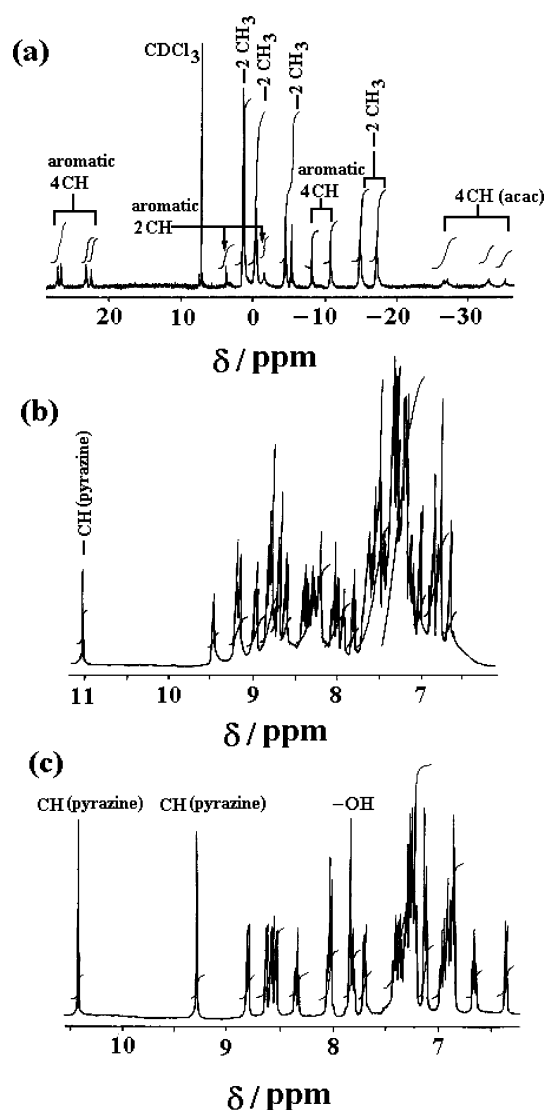


Fig. 2 ^1H NMR spectra of (a) [1] in CDCl_3 , (b) [2](ClO_4) $_2$ and (c) [3](ClO_4) in $(\text{CD}_3)_2\text{SO}$.

corresponding one-electron oxidised $[(\text{bpy})_2\text{Ru}(\mu\text{-L}^{2-})\text{Ru}(\text{bpy})_2]^{3+}$, [4] $^{3+}$, exhibits a K_c value of $10^{2.5}$ for the assumed $\text{Ru}^{\text{II}}\text{Ru}^{\text{III}}$ mixed-valent intermediate. 3d No EPR information was presented to substantiate the mixed-valent assignment in [4] $^{3+}$, an “exceedingly weak feature centred around 2600 nm at the detection limit of the instrument” 3d was invoked for the intervalence charge

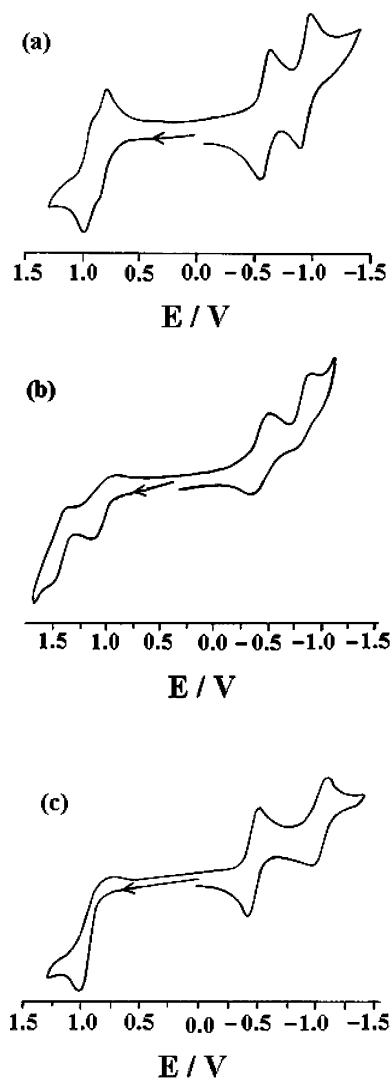


Fig. 3 Cyclic voltammograms of (a) [1], (b) [2](ClO_4) $_2$ and (c) [3](ClO_4) in CH_3CN – $0.1 \text{ mol dm}^{-3} \text{ Et}_4\text{NClO}_4$ at 50 mV s^{-1} .

transfer transition. In any case, the K_c value substantially increases on moving from moderately π -acidic bpy ($10^{2.5}$ for [4] $^{3+}$) to electronically rich σ -donating acac $^-$ ($10^{5.8}$ for [1] $^-$) ancillary ligands as has been noted earlier in analogous systems. 5,11

Table 1 Redox potentials of complexes a

n/n^{-1b}	Couple	$E_{1/2}^c/\text{V}$ ($\Delta E_{pp}/\text{mV}$)	Couple	$E_{1/2}^c/\text{V}$ ($\Delta E_{pp}/\text{mV}$)	Couple	$E_{1/2}^c/\text{V}$ ($\Delta E_{pp}/\text{mV}$)
4/3			$2^{4+}/2^{3+}$	1.45(110)		
3/2			$2^{3+}/2^{2+}$	1.05(100)		
2/1	$1^{2+}/1^+$	0.97(65)	$2^{2+}/2^+$	−0.47(120)	$3^{2+}/3^+$	0.88 d
1/0	$1^+/1$	0.83(65)	$2^+/2$	−0.84(130)	$3^+/3$	−0.47(100)
0/−	$1/1^-$	−0.58(87)			$3/3^-$	−1.00(120)
−2/−	$1^-/1^{2-}$	−0.92(88)				
2/−3−						

a From cyclic voltammetry in CH_3CN – $0.1 \text{ mol dm}^{-3} \text{ Et}_4\text{NClO}_4$ at 50 mV s^{-1} . b Charge change of the $[\text{Ru}(\mu\text{-L}^{2-})\text{Ru}]^{(n/n-1)+}$ core. c In V versus SCE; peak potential differences ΔE_{pp} in mV (in parentheses). d Anodic peak potential (E_{pa}) due to irreversible nature of the voltammogram.

The observed EPR spectra for the odd-electron intermediates at 4 K (Fig. 4b and c) [1^+ : $g_1 = 2.313$, $g_2 = 2.19$, $g_3 = 1.833$; $\Delta g = 0.480$; $g_{av} = 2.122$, and 1^- : $g_1 = 2.316$, $g_2 = 2.150$, $g_3 = 1.760$; $\Delta g = 0.556$; $g_{av} = 2.088$] indicate metal-based spin, effectively low-spin Ru^{III} ,⁹ in both instances. Oxidation is accompanied by the formation of a small amount of radical-type EPR signal at $g = 2.004$ (Fig. 4b), attributed to a free phenoxyl form^{12,13} of the ligand.

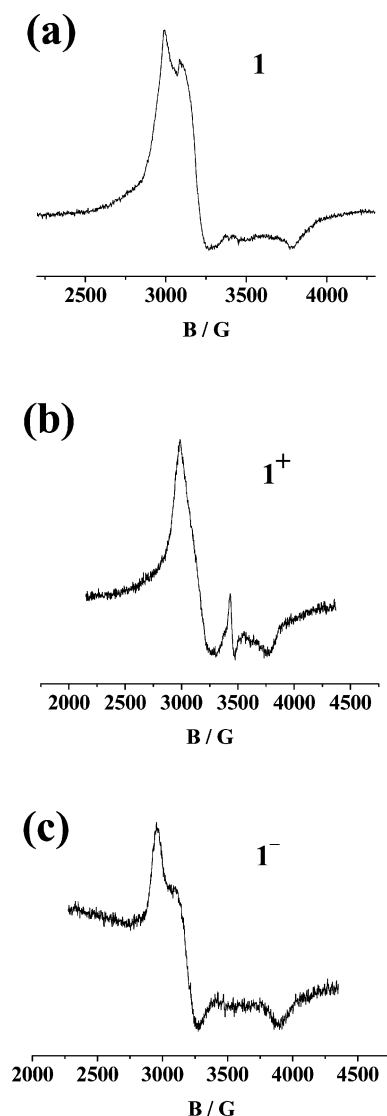


Fig. 4 EPR spectra of (a) $[1]$, (b) $[1]^+$ (free phenoxyl signal from slow decomposition) and (c) $[1]^-$ in $CH_3CN-0.1 \text{ mol dm}^{-3} Bu_4NPF_6$ at 4 K.

Reduction to $[1]^-$ is likely to produce a $Ru^{III}Ru^{II}$ mixed-valent species. The alternative reduction of the L^{2-} bridge is considered less likely because of the rather negative reduction potential of pyrazine⁶ which would be further shifted through substitution with two electron releasing phenolate groups. Compared to free 1,2,4,5-tetrazines,^{14a} the reduction of free pyrazine is shifted cathodically by about 1.5 V.⁶

Oxidation may involve the metal(s), leading to a $Ru^{IV}Ru^{III}$ situation (d^4d^5 mixed-valent configuration), or it may occur at a phenolate, leading to a phenoxyl-type ligand.⁵ Phenoxyl radicals bound to paramagnetic transition metals have been studied

intensively¹² because iron centres in ribonucleotide reductase^{13a} and a copper(II) centre in galactose oxidase exhibit corresponding interactions with the tyrosyl radical.^{13b} In the present case, the three-spin interaction^{14b} in the system $Ru^{III}(\text{phenoxyl})Ru^{III}$ would possibly create metal-based spin ($S = 1/2$) through antiferromagnetic interaction in an alternating up,down,up spin situation.^{14b} UV-VIS-NIR spectroelectrochemistry was thus used to resolve the question of ligand- or metal-based oxidation.

On oxidation of $[1]$ to $[1]^+$ the intensity of the phenolato-to- Ru^{III} based LMCT band (shoulder at 485 nm) decreases with the concomitant growth of several broad absorption features at 655 and 925 nm and a shoulder at 1285 nm (Table 2, Fig. 5a). Most notably, there is no distinct absorption around 480 nm emerging which would indicate the formation of a phenoxyl radical.^{5,12,13} We thus favour a $Ru^{IV}(L^{2-})Ru^{III}$ formulation over the $Ru^{III}(L^{\bullet-})Ru^{III}$ alternative. On second oxidation to $[1]^{2+}$, the intensity of the long-wavelength bands increases further (Table 2, Fig. 5b), ruling out their assignment to IVCT transitions. Instead, these absorptions are attributed to LMCT transitions (phenolato $\rightarrow Ru^{IV}$ or Ru^{III}),

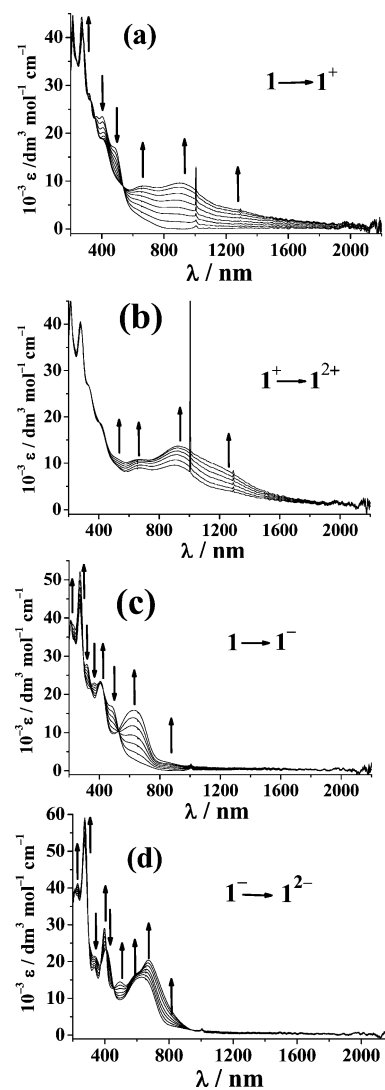


Fig. 5 UV-VIS-NIR spectroelectrochemistry of the conversions of (a) $[1] \rightarrow [1]^+$, (b) $[1]^+ \rightarrow [1]^{2+}$, (c) $[1] \rightarrow [1]^-$ and (d) $[1]^- \rightarrow [1]^{2-}$ in $CH_3CN-0.1 \text{ mol dm}^{-3} Bu_4NPF_6$.

Table 2 UV-VIS-NIR data of complexes in various oxidation states from OTTLE spectroelectrochemistry in CH_3CN –0.1 mol dm^{-3} Bu_4NPF_6

Compound	$\lambda_{\text{max}}/\text{nm}$ ($\epsilon/\text{dm}^3 \text{ mol}^{-1} \text{ cm}^{-1}$)
1^{2+}	1200sh, 925 (13800), 655 (10900), 515sh, 420sh, 335 (26500), 280 (39600), 212 (44700)
1^+	1285sh, 905 (9600), 665 (9000), 405 (18800), 340 (26300), 278 (40500), 213 (44600)
1	625sh, 485 (17000), 403 (23100), 366 (23000), 320 (27900), 271 (43000), 212 (39400)
1^-	865sh, 630 (15900), 407 (23500), 340 (21500), 310sh, 273 (52100), 230sh, 210 (39300)
1^{2-}	800sh, 673 (20400), 585sh, 495 (14500), 397 (29100), 334 (18500), 275 (59100), 230 (41100)
2^{2+}	539 (14600), 355 (32700), 307 (33600), 220 (38900)
2^+	2085 (1600), 910sh, 585 (11900), 490sh, 350 (39300), 262sh, 220 (38400)
2	1050 (9800), 715sh, 611 (6200), 495sh, 445sh, 357 (49400), 240sh, 218 (40800)
3^+	700sh, 590sh, 479 (9900), 345 (31800), 296 (31400), 213 (41200)
3	1915 (950), 792 (1600), 600sh, 466 (10500), 375sh, 342 (32900), 300 (30900), 258 (30800), 212 (41000)
3^-	1045 (7000), 710sh, 535sh, 425 (19300), 346 (42300), 302sh, 250 (33800), 211 (42800)

shifted to lower energies. The IVCT transitions, expected for a $\text{Ru}^{\text{IV}}\text{Ru}^{\text{III}}$ intermediate, are not observed until 2500 nm. However, an IVCT transition for a $\text{Ru}^{\text{IV}}\text{Ru}^{\text{III}}$ mixed-valent state has been detected recently in $[(\text{acac})_2\text{Ru}^{\text{III}}(\mu\text{-gbha}^{2-})\text{Ru}^{\text{IV}}(\text{acac})_2]^+$ ($\text{gbha}^{2-} = 1,4\text{-bis}(2\text{-phenolato})\text{-}1,4\text{-diazabutadiene}$).¹⁵

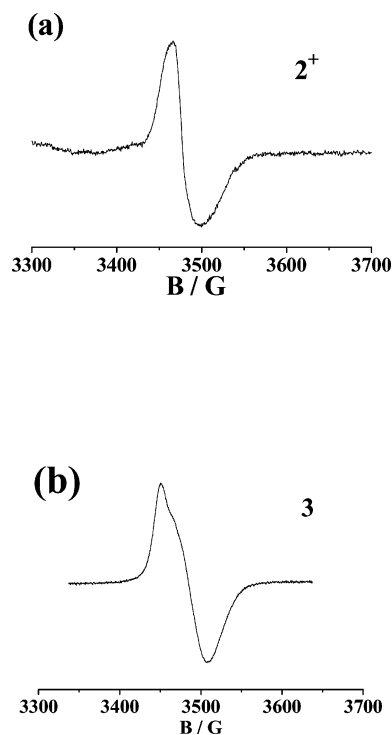
On one-electron reduction of **[1]** to the $\text{Ru}^{\text{III}}\text{Ru}^{\text{II}}$ state in $[\mathbf{1}]^-$ the intensity of the phenolato-to- Ru^{III} LMCT transition is reduced and a new strong band appears at 630 nm, probably due to an MLCT transition Ru^{II} -to- $\pi^*(\text{pyrazine})$. As for $[\mathbf{1}]^+$ the IVCT transition for $[\mathbf{1}]^-$ was not detected up to 2500 nm (Table 2, Fig. 5c). Similar features of considerable electrochemical coupling but without any detectable IVCT transition in the near-IR region have been experienced recently in other $\text{Ru}^{\text{III}}\text{Ru}^{\text{II}}$ mixed-valent systems containing acac^- as ancillary ligand.^{11a-c} Moreover, the analogous complex $[(\text{bpy})_2\text{Ru}^{\text{II}}(\mu\text{-L}^{2-})\text{Ru}^{\text{III}}(\text{bpy})_2]^{3+}$, **[4]**³⁺, was reported to exhibit an “exceedingly weak” IVCT feature just at the detection limit of the instrument around 2600 nm.^{3d} In the absence of detectable IVCT absorptions further speculation on the valence delocalisation (“Class II” or “Class III”)^{2a} is not warranted. On further reduction from $[\mathbf{1}]^-$ to the $\text{Ru}^{\text{II}}\text{Ru}^{\text{II}}$ state in $[\mathbf{1}]^{2-}$ the MLCT band is red-shifted to 673 nm with enhancement of intensity, in accordance with the assignment (Table 2, Fig. 5d). We therefore conclude that the electron transfer in system $[\mathbf{1}]^n$ is exclusively metal-centred, yielding mixed-valent intermediates without detectable IVCT features but with metal-based spin.

With pap as ancillary ligands, the dinuclear complex ion $[\mathbf{2}]^{2+}$ shows two quasi-reversible oxidation and reduction waves in the cyclic voltammogram. The mononuclear $[\mathbf{3}]^+$ exhibits two reversible reductions and one irreversible oxidation process (Table 1, Fig. 3b and 3c). The stabilisation of the ruthenium(II) state is demonstrated by the ~ 1.5 V shift for the $\text{Ru}^{\text{II}}/\text{Ru}^{\text{III}}$ transition on switching from σ -donating acac^- in **[1]** to strongly π -acidic pap in $[\mathbf{2}]^{2+}$. The system $[\mathbf{4}]^{n+}$ with moderately π -acidic bpy ^{3d} takes a middle position. Strong $d\pi(\text{Ru}^{\text{II}}) \rightarrow \pi^*(\text{azo, pap})$ back-bonding in combination with the electrostatic effect is responsible for the destabilisation of Ru^{III} in $[\mathbf{2}]^{2+}$. The 400 mV potential separation for the two oxidation steps of $[\mathbf{2}]^{2+}$ results in a K_{e} value of $10^{6.7}$ for $[\mathbf{2}]^{3+}$ —a larger value than for $[\mathbf{1}]^-$ ($10^{5.8}$) or $[\mathbf{4}]^{3+}$ ($10^{2.5}$) despite the weaker donor and stronger acceptor properties of pap. This result already indicates that the intermediate $[\mathbf{2}]^{3+}$ is not a mixed-valent complex like $[\mathbf{1}]^-$ or $[\mathbf{4}]^{3+}$ but a radical species.

In fact, the *in situ* oxidation of $[\mathbf{2}]^{2+}$ produces a narrow but unresolved EPR signal at $g = 2.0027$, indicative of an organic radical. However, the signal is detectable only at 4 K, suggesting close lying excited states which facilitate relaxation. UV-VIS-

NIR spectroelectrochemistry of $[\mathbf{2}]^{2+}$ starts with a spectrum with a strong MLCT band ($d\pi\text{Ru} \rightarrow \pi^*(\text{pap})$) at 539 nm to produce a broad band at about 1350 nm on oxidation (Table 2, Fig. 7a). However, the oxidation is not fully reversible on the timescale of the spectroelectrochemistry experiment which, like the irreversible oxidation of $[\mathbf{3}]^+$, lends further support to assuming a radical (phenoxyl) species centred on the bridge in $[(\text{pap})_2\text{Ru}^{\text{II}}(\mu\text{-L}^{2-})\text{Ru}^{\text{II}}(\text{pap})_2]^{3+}$,⁵ the remaining MLCT band obscures any expected phenoxyl radical absorption in that region.

Both $[\mathbf{2}]^{2+}$ and $[\mathbf{3}]^+$ display two successive reductions (Table 1, Fig. 3b and 3c). In both cases the first step is considered to be associated with the electron addition to the azo function of one of the pap ligands. Evidence comes from EPR spectroscopy which shows signals at room temperature and at 110 K at $g_{\text{iso}} = 1.980$ (broad, unresolved, Fig. 6a) for $[\mathbf{2}]^+$ and at $g_{\parallel} = 1.985$ and $g_{\perp} = 1.966$ ($\Delta g = 0.019$; $g_{\text{av}} = 1.978$) for **[3]** (Fig. 6b). These values

**Fig. 6** EPR spectra of (a) $[\mathbf{2}]^+$ and (b) **[3]** in CH_3CN –0.1 mol dm^{-3} Bu_4NPF_6 at 110 K.

slightly below 2 are typical for ruthenium(II) complexes of anion radical ligands.¹⁶

On one-electron reduction of $[2]^{2+}$ to the radical species $[(pap^{\bullet-})(pap)Ru^{II}(\mu-L^2-)Ru^{II}(pap)_2]^+$, $[2]^+$, the MLCT band is slightly red-shifted to 585 nm with decrease in intensity. In addition it shows two weak absorptions at 910 and 2085 nm (Table 2, Fig. 7b). These could be partially ascribed to ligand-to-ligand intervalence charge transfer (LLIVCT) transitions between singly occupied and empty π^* orbitals of pap at the same or at different metal centres. The former is supported by a near-IR absorption of mononuclear $[(pap^{\bullet-})(pap)Ru^{II}(HL^-)]$, $[3]$, at 1915 nm (Table 2, Fig. 8a). Relative to $[3]^+$ with MLCT bands at 479, 590 and 760 nm the reduced form $[3]$ exhibits red-shifted bands 466, 600 and 792 nm (Table 2, Fig. 8a).

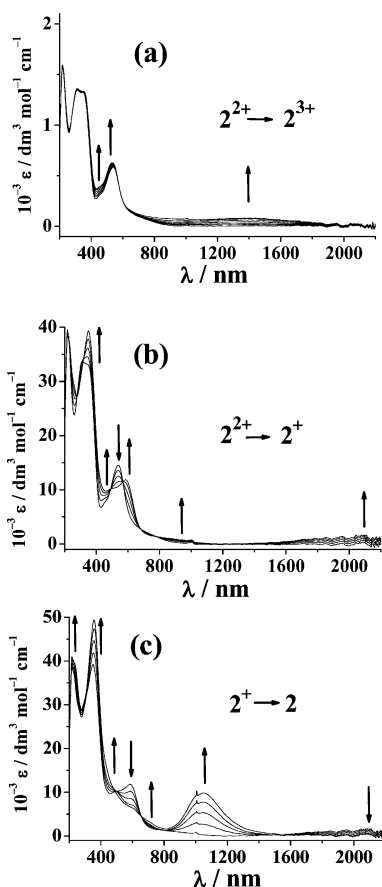


Fig. 7 UV-VIS-NIR spectroelectrochemistry of the conversions of (a) $[2]^{2+} \rightarrow [2]^{3+}$, (b) $[2]^{2+} \rightarrow [2]^+$ and (c) $[2]^+ \rightarrow [2]$ in $CH_3CN-0.1 \text{ mol dm}^{-3} Bu_4NPF_6$.

On second reduction to $[2]$ the MLCT band is red-shifted further to 611 nm with substantial reduction in intensity (Table 2, Fig. 7c). In addition, the intensity of the LLIVCT absorption around 2085 nm decreases and a new intense band appears at 1050 nm in what is formulated as $[(pap^{\bullet-})(pap)Ru^{II}(\mu-L^2-)Ru^{II}(pap)(pap^{\bullet-})]$. Similarly, for $[3]^-$ the intensity of the 1915 nm band decreases and a moderately intense absorption develops at 1045 nm (Table 2, Fig. 8b). This parallel shows an intrinsic similarity which disfavors major bridge-mediated metal-metal communication but illustrates typical absorptions of the common chromophore involving the pap radical anion.

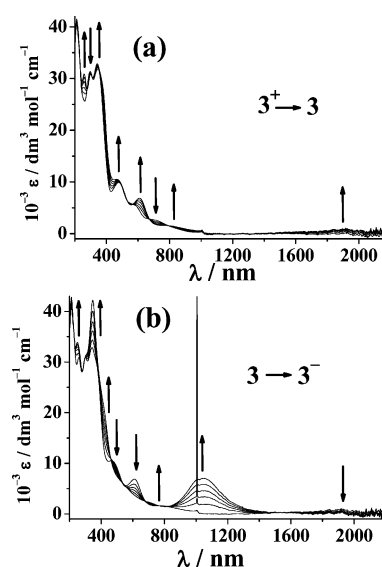


Fig. 8 UV-VIS-NIR spectroelectrochemistry of the conversions of (a) $[3]^+ \rightarrow [3]$ and (b) $[3] \rightarrow [3]^-$ in $CH_3CN-0.1 \text{ mol dm}^{-3} Bu_4NPF_6$.

Using a donor-acceptor modified symmetrical pyrazine as bridge and two very different ancillary ligands, *viz.*, donating $acac^-$ and strongly π accepting pap, we have demonstrated the wide variety of accessible oxidation state combinations in dinuclear ruthenium complexes. Whereas the $[(acac)_2Ru(\mu-L)Ru(acac)_2]^n$ redox system involves only metal-based electron transfer, including the formation of mixed-valent intermediates with ruthenium-centred spin but without detectable intervalence charge transfer bands, the corresponding $[(pap)_2Ru(\mu-L)Ru(pap)_2]^n$ system retains the ruthenium(II) oxidation state and shows electron transfer to the ancillary pap ligands or from the phenolate part of L^{2-} with ligand-centred spin. Non-innocent behaviour of ligands¹⁷ can obviously occur both for bridges and for terminal ligands in dinuclear complexes, complementing the option of mixed-valency for electron transfer. The significance of ancillary ligands in determining the metal oxidation state preference and thus the oxidation state combination in more complex systems can thus not be underestimated.

Experimental

Materials

The starting materials $Ru(acac)_2(CH_3CN)_2$,¹⁸ *etc.* $Ru(pap)_2Cl_2$ ¹⁹ and 2,5-bis(2-hydroxyphenyl)pyrazine = H_2L were prepared according to the reported procedures.^{3d} 4-Hydroxycoumarin was obtained from Aldrich, other chemicals and solvents were reagent grade and used as received. For spectroscopic and electrochemical studies HPLC grade solvents were used.

Physical measurements

UV-VIS-NIR spectroelectrochemical studies were performed in $CH_3CN-0.1 \text{ mol dm}^{-3} Bu_4NPF_6$ at 298 K using an optically transparent thin layer electrode (OTTLE) cell²⁰ mounted in the sample compartment of a J & M TIDAS spectrophotometer. FT-IR spectra were taken on a Nicolet spectrophotometer with samples prepared as KBr pellets. Solution electrical conductivity

was checked using a Systronic 305 conductivity bridge. Magnetic susceptibility was measured with a CAHN electrobalance 7550. ^1H -NMR spectra were obtained with a 300 MHz Varian FT spectrometer. The EPR measurements were made in a two-electrode capillary tube¹⁶ with a X-band Bruker system ESP300, equipped with a Bruker ER035M gaussmeter and a HP 5350B microwave counter. Cyclic voltammetric, differential pulse voltammetric and coulometric measurements were carried out using a PAR model 273A electrochemistry system. Platinum wire working and auxiliary electrodes and an aqueous saturated calomel reference electrode (SCE) were used in a three-electrode configuration. The supporting electrolyte was Et_4NClO_4 and the solute concentration was $\sim 10^{-3} \text{ mol dm}^{-3}$. The half-wave potential $E_{0.298}^{\circ}$ was set equal to $0.5(E_{\text{pa}} + E_{\text{pc}})$, where E_{pa} and E_{pc} are anodic and cathodic cyclic voltammetric peak potentials, respectively. A platinum wire gauze working electrode was used in coulometric experiments. All experiments were carried out under a dinitrogen atmosphere. Elemental analyses were carried out with a Perkin-Elmer 240C elemental analyser. Electrospray mass spectra were recorded on a Micromass Q-ToF mass spectrometer.

Syntheses

CAUTION! Perchlorate salts of metal complexes are generally explosive. Care should be taken while handling such complexes.

[(acac)₂Ru^{III}(μ -L²⁻)Ru^{III}(acac)₂] [1]. The starting complex $[\text{Ru}(\text{acac})_2(\text{CH}_3\text{CN})_2]$ (100 mg, 0.26 mmol), 3,6-bis(2-hydroxyphenyl)pyrazine (H_2L) (34.00 mg, 0.13 mmol) and sodium acetate 21.0 mg, (0.26 mmol) were taken in 20 cm³ ethanol and the mixture was heated at reflux for 12 h. The initially orange solution gradually turned dark. The solvent was then removed under reduced pressure. The solid mass thus obtained was purified by using a silica gel (60–120 mesh) column. Initially a red solution corresponding to $\text{Ru}(\text{acac})_3$ was obtained by elution with CH_2Cl_2 – CH_3CN (50 : 1). With CH_2Cl_2 – CH_3CN (10 : 1), a dark brown solution corresponding to [1] was then separated. Evaporation of solvent under reduced pressure afforded complex [1]. Yield: 62 mg (55.00%). Anal. Calcd for [1]: C, 49.90; H, 4.55; N, 3.54. Found: C, 50.11; H, 4.44; N, 3.25%. ^1H NMR (CDCl_3): δ (ppm) (J/Hz): 27.18 (CH, aromatic), 26.75 (CH, aromatic), 23.19 (CH, aromatic), 22.49 (CH, aromatic), 3.48 (CH, aromatic), –1.57 (CH, aromatic), –8.12 (2CH, aromatic), –10.78 (2CH, aromatic), 1.26 (2CH₃(acac)), –0.31 (CH₃(acac)), –0.48 (CH₃(acac)), –4.49 (CH₃(acac)), –5.32 (CH₃(acac)), –14.89 (CH₃(acac)), –17.23 (CH₃(acac)), –26.64 (CH(acac)), –27.48 (CH(acac)), –32.90 (CH(acac)), –35.32 (CH(acac)).

[(pap)₂Ru(μ -L²⁻)Ru(pap)₂](ClO₄)₂, [2](ClO₄)₂, and [(pap)₂Ru(HL⁻)](ClO₄)₂, [3](ClO₄)₂. *cis*- $[\text{Ru}(\text{pap})_2\text{Cl}_2]$ (100 mg; 0.186 mmol) and AgClO_4 (100 mg; 0.48 mmol) were heated to reflux in 10 cm³ of ethanol for 2 h under a dinitrogen atmosphere. The precipitated AgCl was filtered off yielding $[\text{Ru}(\text{pap})_2(\text{EtOH})_2]^{2+}$. To this, H_2L (24.00 mg, 0.09 mmol) and sodium acetate (25 mg; 0.30 mmol) were added and the mixture was refluxed for 15 h under dinitrogen. The purple solution thus obtained was evaporated to dryness under reduced pressure and purified by column chromatography using a silica gel column (60–120 mesh). With CH_2Cl_2 – CH_3CN (5 : 1) a brown solution corresponding to mononuclear [3](ClO₄) was eluted

initially, followed by a purple solution corresponding to dinuclear [2](ClO₄)₂ as separated by CH_2Cl_2 – CH_3CN (4 : 1). Evaporation of solvents under reduced pressure afforded pure complexes [3](ClO₄) and [2](ClO₄)₂.

For [2](ClO₄)₂. Yield: 51 mg (40%); Anal. Calcd: C, 51.57; H, 3.32; N, 14.04. Found: C, 51.90; H, 2.96; N, 14.29%. A_{M} ($\Omega^{-1} \text{ cm}^2 \text{ mol}^{-1}$) in acetonitrile at 298 K: 239. ^1H NMR ($(\text{CD}_3)_2\text{SO}$), δ (ppm) (J/Hz): 11.05 (s, 2CH, pyrazine), 9.47 (d, 4.4, 1H), 9.21 (t, 5.6, 5.6, 2H), 8.99 (t, 6.0, 8.8, 2H), 8.82 (m, 3H), 8.71 (d, 8.0, 2H), 8.62 (t, 8.8, 8.0, 1H), 8.32 (m, 5H), 8.05 (m, 3H), 7.94 (t, 6.4, 6.4, 1H), 7.83 (t, 4.8, 8.0, 1H), 7.62 (m, 6H), 7.44 (m, 9H), 7.03 (d, 7.2, 1H), 6.88 (t, 8.0, 7.2, 2H), 6.79 (t, 8.8, 7.2, 2H), 6.66 (d, 6.4, 2H), 6.59 (d, 7.2, 1H).

For [3](ClO₄)₂. Yield: 30 mg (20%); Anal. Calcd: C, 54.93; H, 3.52; N, 13.50. Found: C, 54.56; H, 3.41; N, 13.37%. A_{M} ($\Omega^{-1} \text{ cm}^2 \text{ mol}^{-1}$) in acetonitrile at 298 K: 138. ^1H NMR ($(\text{CD}_3)_2\text{SO}$), δ (ppm) (J/Hz): 10.43 (s, CH, pyrazine, 1H), 9.28 (s, CH, pyrazine, 1H), 8.8 (d, 8.0, 1H), 8.63 (d, 5.0, 1H), 8.58 (d, 8.0, 1H), 8.35 (d, 8.0, 1H), 8.34 (t, 8.0, 8.0, 1H), 8.04 (t, 7.2, 8.0, 2H), 7.84 (s, OH, 1H), 7.81 (t, 6.8, 6.0, 1H), 7.70 (d, 8.0, 1H), 7.32 (m, 7H), 7.13 (d, 8.0, 2H), 6.92 (m, 5H), 6.66 (t, 8.0, 7.2, 1H), 6.35 (d, 8.0, 1H).

X-Ray crystal structure analysis

Yellow single-crystals of $\text{H}_2\text{boppz} = \text{H}_2\text{L}$ were grown by slow evaporation of a DMSO solution of the compound. X-Ray diffraction data were collected on a PC-controlled Enraf-Nonius CAD-4 (MACH-3) single-crystal X-ray diffractometer by using MoK_α radiation. The structure was solved and refined (full-matrix least-squares on F^2) by using the SHELX-97 (SHELXTL) program package.²¹ Hydrogen atoms were included in the refinement process as per the riding model.

Molecular formula: $\text{C}_{16}\text{H}_{12}\text{N}_2\text{O}_2$. Crystal symmetry: monoclinic; space group: $P2_1/n$; $a/\text{\AA}$: 5.9660(7); $b/\text{\AA}$: 3.8840(5); $c/\text{\AA}$: 26.330(2); $\beta/^\circ$: 94.788(8); $V/\text{\AA}^3$: 607.99(12); Z : 2; μ/mm^{-1} : 0.097; T/K : 293(2); $D_{\text{calcd}}/\text{g cm}^{-3}$: 1.444; $F(000)$: 276; 2θ range/ $^\circ$: 3.10 to 49.90; e -data (R_{int}): 1055 [$R(\text{int}) = 0.0357$]; $R1$, $wR2$ [$I > 2\sigma(I)$]: 0.0517, 0.0972; GOF: 0.983; largest diff. peak and hole/ $e \text{\AA}^{-3}$: 0.199 and –0.217.

CCDC reference number 6355245.

For crystallographic data in CIF or other electronic format see DOI: 10.1039/b701511a

Acknowledgements

Financial support received from the Department of Science and Technology and Council of Scientific and Industrial Research, New Delhi (India), the DAAD, the DFG and the FCI (Germany) is gratefully acknowledged.

References

- (a) J.-P. Launay, *Chem. Soc. Rev.*, 2001, **30**, 386; (b) S. B. Brunschwig, C. Creutz and N. Sutin, *Chem. Soc. Rev.*, 2002, **31**, 168; (c) K. D. Demadis, C. M. Hartshorn and T. J. Meyer, *Chem. Rev.*, 2001, **101**, 2655; (d) W. Kaim, A. Klein and M. Glöckle, *Acc. Chem. Res.*, 2000, **33**, 755; (e) J. A. McCleverty and M. D. Ward, *Acc. Chem. Res.*, 1998, **31**, 842; (f) D. Astruc, *Acc. Chem. Res.*, 1997, **30**, 383; (g) M. D. Ward, *Chem. Soc. Rev.*, 1995, **24**, 121; (h) G. Giuffrida and S. Campagna, *Coord. Chem. Rev.*, 1994, **135–136**, 517; (i) R. J. Crutchley, *Adv. Inorg. Chem.*, 1994, **41**, 273;

- (j) R. J. Crutchley, G. P. A. Yap and M. Al-Noaimi, *Inorg. Chem.*, 2004, **43**, 1770; (k) N. Shan, S. J. Vickers, H. Adams, M. D. Ward and J. A. Thomas, *Angew. Chem., Int. Ed.*, 2004, **43**, 3938; (l) R. H. Laye, S. M. Couchman and M. D. Ward, *Inorg. Chem.*, 2001, **40**, 4089; (m) W. E. Meyer, A. J. Amoroso, C. R. Horn, M. Jaeger and J. A. Gladysz, *Organometallics*, 2001, **20**, 1115; (n) J. E. Ritchie and R. W. Murray, *J. Am. Chem. Soc.*, 2000, **122**, 2964; (o) T. Weyland, K. Coustas, L. Toupet, J. F. Halet and C. Lapinte, *Organometallics*, 2000, **19**, 4228.
- 2 (a) C. Creutz, *Prog. Inorg. Chem.*, 1983, **30**, 1; (b) M. Sommovigo, G. Denti, S. Serroni, S. Campagna, C. Mingazzini, C. Mariotti and A. Juris, *Inorg. Chem.*, 2001, **40**, 3318; (c) S. Campagna, G. Denti, G. D. Rosa, L. Sabatino, M. Ciano and V. Balzani, *Inorg. Chem.*, 1989, **28**, 2565; (d) G. Denti, S. Campagna, L. Sabatino, S. Serroni, M. Ciano and V. Balzani, *Inorg. Chem.*, 1990, **29**, 4750; (e) P. Ceroni, F. Paolucci, C. Paradisi, A. Juris, S. Roffia, S. Serroni, S. Campagna and A. J. Bard, *J. Am. Chem. Soc.*, 1998, **120**, 5480; (f) R. W. Callahan, F. R. Keene, T. J. Meyer and D. J. Salmon, *J. Am. Chem. Soc.*, 1977, **99**, 1064; (g) R. Hage, H. E. B. Lempers, J. G. Haasnoot and J. Reedijk, *Inorg. Chem.*, 1997, **36**, 3139; (h) C. Creutz and H. Taube, *J. Am. Chem. Soc.*, 1969, **91**, 3988; (i) D. E. Richardson and H. Taube, *J. Am. Chem. Soc.*, 1983, **105**, 40; (j) D. E. Richardson and H. Taube, *Coord. Chem. Rev.*, 1984, **60**, 107; (k) P. A. Lay, R. H. Magnuson and H. Taube, *Inorg. Chem.*, 1988, **27**, 2364.
- 3 (a) T. E. Keyes, B. Evrard, J. G. Vos, C. Brady, J. J. McGarvey and P. Jayaweera, *Dalton Trans.*, 2004, 2341; (b) S. Chakraborty, R. H. Laye, P. Munshi, R. L. Paul, M. D. Ward and G. K. Lahiri, *J. Chem. Soc., Dalton Trans.*, 2002, 2348; (c) S. Chakraborty, R. H. Laye, R. L. Paul, R. G. Gonnade, V. G. Puranik, M. D. Ward and G. K. Lahiri, *J. Chem. Soc., Dalton Trans.*, 2002, 1172; (d) I. Brady, D. Leane, H. P. Hughes, R. J. Foster and T. E. Keyes, *Dalton Trans.*, 2004, 334.
- 4 P. J. Mosher, G. P. A. Yap and R. J. Crutchley, *Inorg. Chem.*, 2001, **40**, 1189.
- 5 S. Patra, B. Sarkar, S. Maji, J. Fiedler, F. A. Urbanos, R. Jimenez-Aparicio, W. Kaim and G. K. Lahiri, *Chem.–Eur. J.*, 2006, **12**, 489.
- 6 W. Kaim, *Angew. Chem.*, 1983, **95**, 201, (*Angew. Chem. Int. Ed. Engl.*, 1983, **22**, 171).
- 7 (a) B. K. Santra, G. A. Thakur, P. Ghosh, A. Pramanik and G. K. Lahiri, *Inorg. Chem.*, 1996, **35**, 3050; (b) R. Samanta, B. Mondal, P. Munshi and G. K. Lahiri, *J. Chem. Soc., Dalton Trans.*, 2001, 1827; (c) B. Mondal, H. Paul, V. G. Puranik and G. K. Lahiri, *J. Chem. Soc., Dalton Trans.*, 2001, 481.
- 8 (a) S. Patra, T. A. Miller, B. Sarkar, M. Niemeyer, M. D. Ward and G. K. Lahiri, *Inorg. Chem.*, 2003, **42**, 4707; (b) T. Koiwa, Y. Masuda, J. Shono, Y. Kawamoto, Y. Hoshino, T. Hashimoto, K. Natarajan and K. Shimizu, *Inorg. Chem.*, 2004, **43**, 6215; (c) D. R. Eaton, *J. Am. Chem. Soc.*, 1965, **87**, 3097; (d) R. A. Palmer, R. C. Fay and T. S. Piper, *Inorg. Chem.*, 1964, **3**, 875; (e) R. H. Holm and F. A. Cotton, *J. Am. Chem. Soc.*, 1958, **80**, 5658; (f) R. C. Fay and T. S. Piper, *J. Am. Chem. Soc.*, 1963, **85**, 500; (g) J.-L. Chen, X.-U. Zhang, L.-Y. Zhang, L.-X. Shi and Z.-N. Chen, *Inorg. Chem.*, 2005, **44**, 1037.
- 9 N. Chanda, B. Sarkar, J. Fiedler, W. Kaim and G. K. Lahiri, *Dalton Trans.*, 2003, 3550.
- 10 S. Ghumaan, B. Sarkar, S. Patra, J. van Slageren, J. Fiedler, W. Kaim and G. K. Lahiri, *Inorg. Chem.*, 2005, **45**, 3210.
- 11 (a) S. Patra, B. Sarkar, S. Ghumaan, J. Fiedler, W. Kaim and G. K. Lahiri, *Inorg. Chem.*, 2004, **43**, 6108; (b) S. Patra, B. Sarkar, S. Ghumaan, J. Fiedler, W. Kaim and G. K. Lahiri, *Dalton Trans.*, 2004, 754; (c) S. Patra, B. Sarkar, S. Ghumaan, J. Fiedler, S. Zalis, W. Kaim and G. K. Lahiri, *Dalton Trans.*, 2004, 750; (d) S. Ghumaan, B. Sarkar, S. Patra, K. Parimal, J. van Slageren, J. Fiedler, W. Kaim and G. K. Lahiri, *Dalton Trans.*, 2005, 706; (e) S. Chellamma and M. Lieberman, *Inorg. Chem.*, 2001, **40**, 3177; (f) S. Kar, B. Sarkar, S. Ghumaan, D. Janardanan, J. van Slageren, J. Fiedler, V. G. Puranik, R. B. Sunoj, W. Kaim and G. K. Lahiri, *Chem.–Eur. J.*, 2005, **11**, 4901; (g) B. Sarkar, S. Patra, J. Fiedler, R. B. Sunoj, D. Janardanan, S. M. Mobin, M. Niemeyer, G. K. Lahiri and W. Kaim, *Angew. Chem., Int. Ed.*, 2005, **44**, 5655.
- 12 P. Chaudhury and K. Wieghardt, *Prog. Inorg. Chem.*, 2001, **50**, 151.
- 13 (a) J. M. Bollinger, Jr., O. E. Edmondson, B. H. Huynh, J. Filley Norton, Jr. and J. Stubbe, *Science*, 1991, **253**, 292; (b) M. Kaupp, T. Gress, R. Reviakine, O. L. Malkina and V. G. Malkin, *J. Phys. Chem. B*, 2003, **107**, 331.
- 14 (a) W. Kaim, *Coord. Chem. Rev.*, 2002, **230**, 126; (b) S. Ye, B. Sarkar, F. Lissner, T. Schleid, J. van Slageren, J. Fiedler and W. Kaim, *Angew. Chem., Int. Ed.*, 2005, **44**, 2103.
- 15 S. Kar, B. Sarkar, S. Ghumaan, D. Roy, F. A. Urbanos, J. Fiedler, R. B. Sunoj, R. Jimenez-Aparicio, W. Kaim and G. K. Lahiri, *Inorg. Chem.*, 2005, **44**, 8715.
- 16 W. Kaim, S. Ernst and V. Kasack, *J. Am. Chem. Soc.*, 1990, **112**, 173.
- 17 M. D. Ward and J. A. McCleverty, *J. Chem. Soc., Dalton Trans.*, 2002, 275.
- 18 T. Kobayashi, Y. Nishina, K. G. Shimizu and G. P. Satô, *Chem. Lett.*, 1988, 1137.
- 19 S. Goswami, A. R. Chakravorty and A. Chakravorty, *Inorg. Chem.*, 1981, **20**, 2246.
- 20 M. Krejčík, M. Danek and F. Hartl, *J. Electroanal. Chem.*, 1991, **317**, 179.
- 21 G. M. Sheldrick, *SHELX-97, Program for Crystal Structure Solution and Refinement*, University of Göttingen, Germany, 1997.